



THE PLEISTOCENE EVOLUTION AND RECONSTRUCTION OF LGM AND LATE GLACIAL PALEOGLACIERS OF THE SILISIA VALLEY AND MOUNT RAUT (CARNIC PREALPS, NE ITALY).

Lukas Rettig¹, Giovanni Monegato², Paolo Mozzi¹, Manja Žebre³,
Luigi Casetta⁴, Michele Ferneti⁴, Renato R. Colucci⁵

¹Dipartimento di Geoscienze, Università di Padova, Padova, Italy.

²CNR - Istituto di Geoscienze e Georisorse, Padova, Italy.

³Geološki zavod Slovenije, Ljubljana, Slovenia.

⁴Dipartimento di Matematica e Geoscienze, Università di Trieste, Trieste, Italy.

⁵CNR - Istituto di Scienze Polari, Venezia-Mestre, Italy.

Corresponding Author: G. Monegato <giovanni.monegato@igg.cnr.it>

ABSTRACT: Small, peripheral mountain glaciers that remained independent from the large ice-streams throughout the Pleistocene glaciations represent an important source of paleoclimatic information in the European Alps. Here, we present new evidence on the evolution of the Silisia Valley and paleoglaciers on the northern side of Mount Raut (Carnic Prealps, NE Italy). The area is characterized by the presence of a variety of sediments and landforms, among them two generations of conglomerates and several deposits of glacial origin. The conglomerates are related to the infill and subsequent incision of the Silisia Valley during Plio (?)–Pleistocene times, whereas most of the glacial deposits can be ascribed to glacier advances during the Last Glacial Maximum (LGM) and following Late Glacial stadials. During the LGM, the glacial system extended from the headwalls of Mount Raut (2026 m a.s.l.) down to an elevation of 440 m, and had an equilibrium line altitude (ELA) of 1260 m (Accumulation-Area-Balance Ratio method - AABR). Assuming present-day amounts of precipitation, this corresponds to a mean summer air temperature (MSAT) depression of 8.5 or 9.4°C ($\sigma = \pm 2.2^\circ\text{C}$), when compared to two recent (1960–1990) climatic records in the area. Two phases of glacier stabilization during the Late Glacial were inferred from frontal moraine systems at higher elevations. During the first one, the glaciers had an ELA of 1590 m (corresponding to an MSAT lowering of 6.2 or 7.1°C), whereas at the second one the ELA was at 1740 m (MSAT lowering of 5.3 or 6.1°C). Our results allow to better understand the long-term Pleistocene evolution of this sector of the south-eastern Alps, probably driven by the interplay between climatic fluctuations and phases of tectonic uplift. We further provide new insights on paleoglaciers of the last glacial cycle that may help in the validation of regional climatic models.

Keywords: Last Glacial Maximum, Carnic Prealps, palaeoglacier reconstruction, equilibrium line altitude, conglomerates.

1. INTRODUCTION

The reconstruction of the Alpine glacier network during the late Pleistocene glaciations has been attempted several times through geomorphological evidence coupled with chronological data (Penck & Brückner, 1901–1909; Castiglioni, 1940; van Husen, 1987; Ehlers & Gibbard, 2004). Alpine-scale models of the last glacial cycle were recently performed (Jouvet et al., 2017; Seguinot et al., 2018), but in several sectors the results are not consistent with the geomorphological evidence. Because of their location at the boundary between the Mediterranean and continental Europe, the Alps show a high climate variability (e.g., Beniston, 2005; Isotta et al., 2014) and are affected by a wide range of air flows and humidity conditions, as sectors of the chain face a continental-type climate and others maritime-type conditions (Beniston, 2006). For this reason, large-scale modelling studies need to be tested in selected areas through paleoclimatic proxies to account

for these regionally-varying climatic conditions. Due to their complex geomorphological and geological structure (Dal Piaz et al., 2003), the external sectors of the Alps are particularly characterized by a large diversity of climatic environments (Ivy-Ochs et al., 2021). A better knowledge of the Pleistocene history of these areas can help to understand the direct relationships between climate change, landscape evolution and the development of glaciers during the cold periods.

During the Last Glacial Maximum (LGM), the Alps hosted the largest ice cap in Europe outside the British and Scandinavian ice sheets (Hughes et al., 2016; Clark et al., 2021 and references therein). In the pre-Alpine belts along the southern side of the Alps, however, also several small and isolated glaciers developed during the LGM (e.g., Carraro & Sauro, 1979; Baratto et al., 2003; Cucato, 2007; Forno et al., 2010; Monegato, 2012). Thanks to their relatively simple geometry, small glaciers permit accurate estimates of their equilibrium line altitude (ELA) that integrate field data with numerical ap-

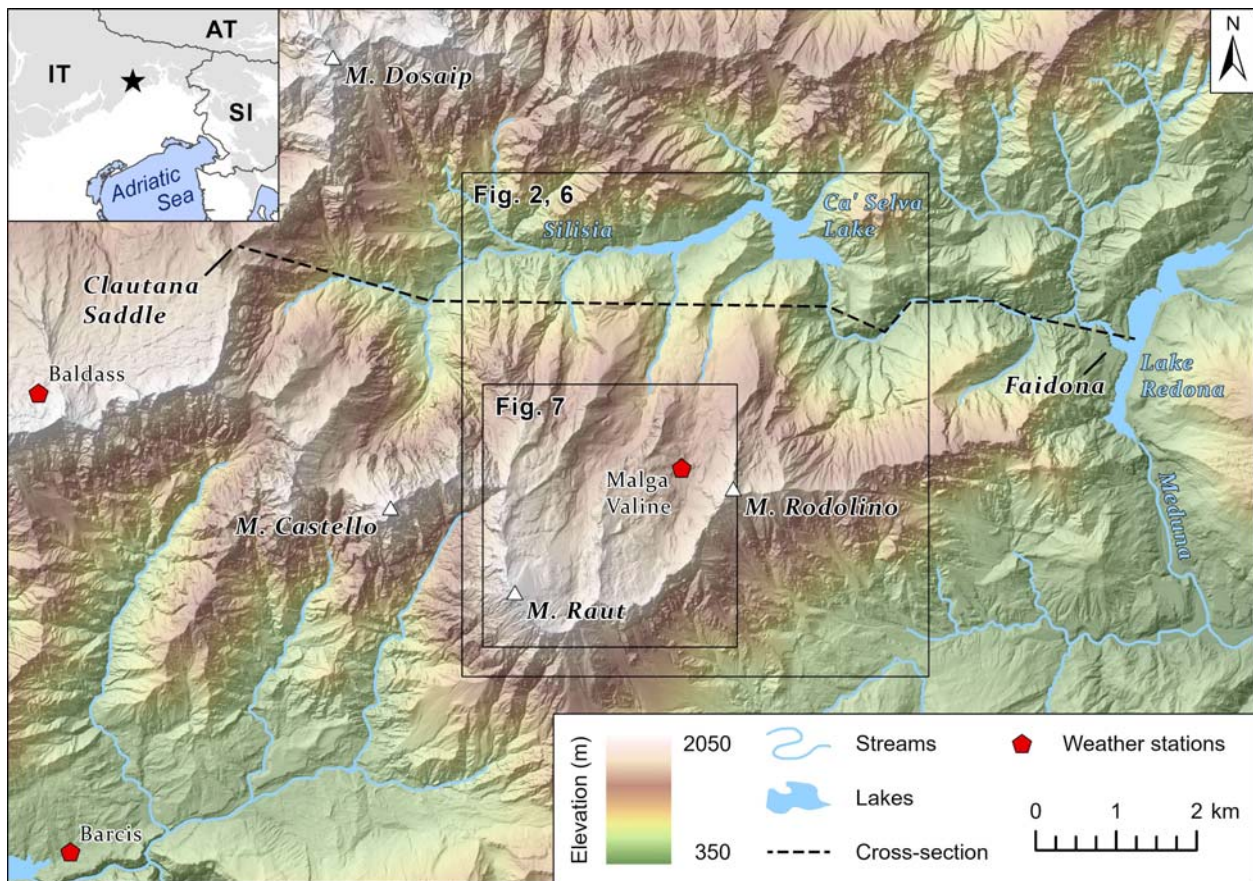


Fig. 1 - Topographic overview of the Mount Raut, the Silisia Valley and its location within the south-eastern Alps. For reference, also the extent of some following figures in the paper (Figs. 2, 6, and 7) is marked here. The underlying DEM was derived from the geoportale of Regione Autonoma Friuli Venezia Giulia (<http://irdat.regione.fvg.it>).

proaches of glacier reconstruction (Pellitero et al., 2015, 2016). For large and interconnected valley glaciers, on the other hand, ELA calculations are still problematic and can only work with models involving the whole mountain range (Kuhlemann et al., 2008; Višnjević et al., 2020), but without detailed field assessments. As the ELA is a parameter that reflects not only local settings but also the regional climate in glaciated areas, its calculation for specific glaciers provides relevant information for inferring robust paleoclimatic reconstructions (e.g., Bacon et al., 2001; Spagnolo & Ribolini, 2019; Rea et al., 2020).

The present work shows, for the first time, the distribution of Quaternary deposits on the northern side of Mount Raut (Carnic Prealps). Due to its location, close to the Friulian piedmont plain, this area is specifically interesting for evaluating the influence of local meteorological factors, such as southerly moisture sources, on the evolution of former glaciations. Through mapping and description of the sedimentary units, both the longer-term Pleistocene evolution of the area and specifically the extent of paleoglaciers during the LGM and two Late Glacial stages are reconstructed. The calculated ELA values of these glaciers are then used to estimate paleoclimatic parameters for the Carnic Prealps and to compare them with other regional climate proxies.

2. GEOMORPHOLOGICAL AND GEOLOGICAL SETTING

The Carnic Prealps (south-eastern European Alps) comprise the drainage basins of the Cellina, Meduna and Arzino streams and reach their maximum elevation in the western sector (Cima dei Preti, 2703 m a.s.l.). Mount Raut is located on the southern fringe of the Carnic Prealps and reaches an elevation of 2026 m (Fig. 1). Its northern and eastern sides are included in the Meduna catchment, while the south-western slope drains towards the Cellina catchment. The northern side of Mount Raut has three major narrow valleys, namely: Valine, Basson and Val Bassa (Fig. 2). All of them are characterized by ephemeral surface runoff because of the karstic landscape (Carulli et al., 2000, 2006). They are tributary valleys of the Silisia valley, nowadays partially drowned by the artificial Ca' Selva Lake. Pre-dam 1:25,000 scale topographic maps show that the presently submerged terminal tracts of the Valine and Basson valley were quite large and flat, with fluvial terraces driven by the incision of the Silisia Stream. The valley heads are characterized by large (2.25 and 1.5 km², respectively) and gently dipping plateaus, located above 1400-1500 m and surrounded by the summit crest of Mount Raut. To the west, the morphology is dominated

by the towering shape of Mount Castello (1923 m) and minor peaks towards the Clautana Saddle (Fig. 1). In this upper sector of the Silisia catchment, valleys are narrow and deeply incised. The northern side of the Silisia Valley comprises the steep walls of Mount Dosaip (2062 m) and minor and low-elevated peaks. The southern slope of the Mount Raut is characterized by 800 to 1200 m high walls dominating the nearby Friulian piedmont plain.

The bedrock in the area of the Mount Raut consists mainly of Jurassic limestones (Calcari Grigi and Vajont Limestone) overlying Late Triassic (Norian-

Rhaetian) dolostones of the Friulian carbonate shelf (Dolomia Principale). Carnian dolostones (Monticello Formation) crop out in the hangingwall of the E-W trending, south-verging Silisia thrust (Fig. 2; Carulli et al., 2000).

The Quaternary deposits are widely distributed and have been mapped only at scales from 1:50,000 to 1:100,000 in the general geological maps of the area (Zenari, 1929; Carulli et al., 2000). More detailed studies are lacking for the Silisia Valley and the Mount Raut, and also the drainage basin of the Meduna is poor in description about the Quaternary succession. Only the

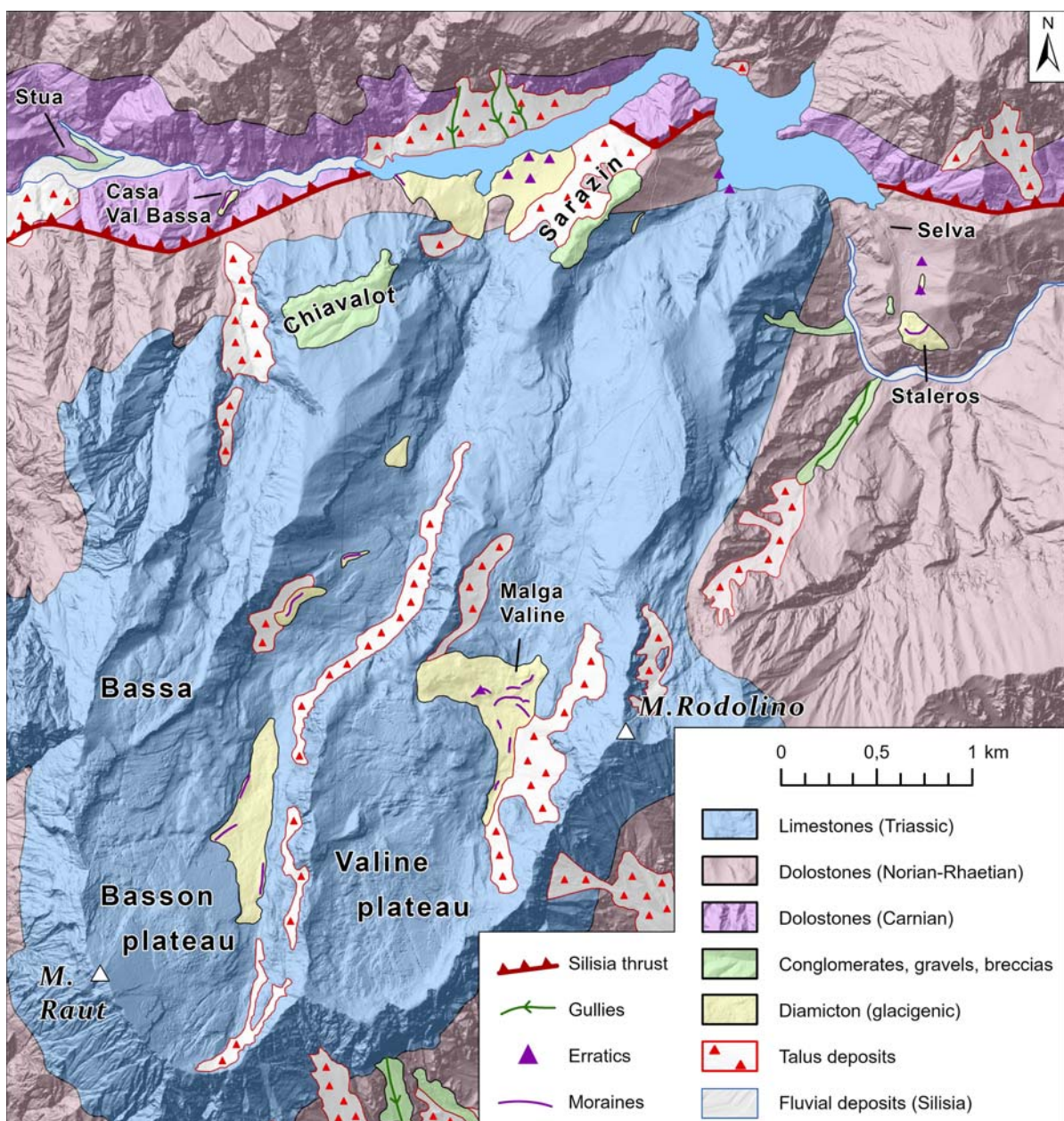


Fig. 2 - Simplified geological map of the northern side of Mount Raut with locations of Quaternary deposits and moraine ridges. Boundaries of geological units and the location of the fault line are from Carulli et al. (2000).

lacustrine deposits of Lake Redona (Venzo et al., 1975; Cavallin & Martinis, 1981) and the complex Quaternary succession in the lower valley reach (Carraro & Polino, 1976; Venturini, 1985; Venturini et al., 2013; Monegato & Poli, 2015) have been studied. As a result of this lack of detailed data, the extent of the Mount Raut paleoglacier during the LGM is still debated. In the early map by Castiglioni (1940) only a small glacier, just reaching the bottom of the Silisia Valley, is shown and the Meduna Valley was considered ice-free. This interpretation was maintained in the most recent CLIMEX map (Vai & Cantelli, 2004). Gortani (1959) reported a larger glacier in the Silisia Valley, merging to that flowing down the Meduna trunk valley. A similar large ice extent, including the Meduna Valley, was reported in the map by Ehlers & Gibbard (2004), following the review by Castiglioni (2004).

The area is presently characterized by a quite high precipitation with constant contribution from all seasons (Crespi et al., 2018). The 1961-2000 climatology at Barcis, according to the local meteorological observatory (www.meteo.fvg.it, last accessed July 9th, 2021), presents mean annual precipitation (MAP) equal to 2197 mm water equivalent (w.e.), with January the driest month (116 mm w.e.) and October the wettest (287 mm w.e.). The impact of moist southerly winds (Scirocco) in the Carnic pre-Alpine sector generally leads to long-lasting orographic precipitation and intense convective systems in all seasons, representing the main driver for such high MAP (Colucci et al., 2021). Recent (2004-2020) mean annual air temperature (MAAT), calculated for the weather station of Pala D'Altei (www.meteo.fvg.it, last accessed July 9th, 2021), located at 1528 m about 8.5 km to the south-west, is equal to 6.4°C, with January and February being the coldest months (-1.5°C) and July the warmest (14.8°C). A longer climatological record has been reconstructed by Colucci & Guglielmin (2015) for the Mount Canin/Kanin (Julian Alps) at an elevation of 2200 m, representing an important regional source of temperature data that precedes the most recent climatic warming since the 1990s.

3. METHODS

Field surveys in the study area were carried out between 2018 and 2021 to describe and map the distribution of geomorphological features and Quaternary deposits along the northern side of Mount Raut and in the Silisia Valley. The mapping procedure was performed on regional topographic maps at a scale of 1:5000, with the support of LiDAR data (grid resolution of 1 m, survey carried on 2006) derived from the geportal of *Regione Autonoma Friuli Venezia Giulia* (<http://irdat.regione.fvg.it>). Older topographic maps (IGM at a scale of 1:25,000) allowed reconstructing the topography of the Silisia Valley prior to the construction of the dam at Ca' Selva.

Based on these elevation data and on the geomorphological and sedimentological evidence found during field work, reconstructions of paleoglacier geometries and ELAs were carried out using recently developed toolboxes within *ESRI ArcMap v. 10.7* (Pellitero et al., 2015, 2016). Glacier surfaces were reconstructed along

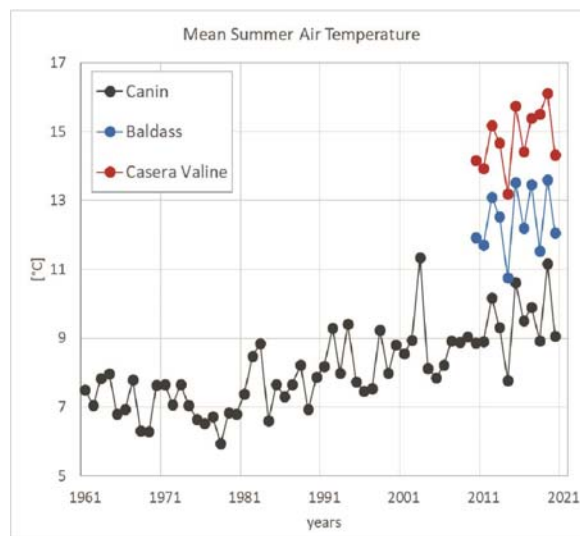


Fig. 3 - Mean summer air temperature (MSAT) at Canin (1961-2020), Baldas (Mount Resettum) and Malga Valine (Mount Raut) (2010-2020) from Colucci and Guglielmin (2015) and www.meteo.fvg.it (last accessed, July 9th 2021). The data demonstrated the close statistical correlation between the three records.

flowlines, extending from mapped moraine ridges or the lower limits of till outcrops up to the accumulation areas on the plateaus at the valley head. Initially, a subglacial shear stress of 100 kPa, characteristic of the base of alpine glaciers, was applied to the whole length of these flowlines (Paterson, 1994; Brædstrup et al., 2016; Pellitero et al., 2016). This value had to be additionally modified in some parts of the catchment, with the aim of better tuning the reconstructed glacier surface with the geomorphological evidence. Generally, the low-lying valley mouths required a lower shear stress (50 kPa) to yield realistic ice-thicknesses, which is compatible with the glacier overriding thicker sediment fills with low yield strength at these locations (Thorp, 1991; Iverson et al., 2003). For the steep glacial troughs of the Basson and Bassa valleys, an additional F-factor adjustment, which is a function of the glacier width and thickness, was applied to account for lateral drag exerted by the valley walls (Nye, 1952; Benn & Hulton, 2010; Pellitero et al., 2016).

From the reconstructed glacier surfaces, ELAs were calculated using both the Accumulation-Area-Balance Ratio (AABR) and the Accumulation-Area-Ratio (AAR), as frequently applied in studies on paleoglaciers in the European Alps (e.g., Federici et al., 2012; Monegato, 2012; Hofmann et al., 2019; Spagnolo & Ribolini, 2019). For the AABR-method, balance ratios of 1.56 (representing a global median value) and 1.29 (representing the median value for modern Alpine glaciers) were chosen (Oien et al., 2021). For the AAR-method, the global median value of 0.58 was initially used (Rea, 2009; Oien et al., 2021), but ELAs were also calculated for ratios of 0.5, 0.65, and 0.7 to test for the sensitivity of reconstructed ELAs on the choice of different AARs.

To facilitate paleoclimate interpretations, present-

day temperature and precipitation in the study area were reconstructed first. This included the 1961-2000 MAP in Barcis and the 2010-2020 Mean Summer Air Temperature (MSAT) at the local weather stations of Malga Valine-Mount Rest (1346 m) and Baldass-Mount Resettum (1817 m), the latter located ca. 6 km to the West of Mount Raut (for location of weather stations see Fig. 1). In order to obtain a MSAT for the climatic period 1961-1990, the values from the local weather stations were then corrected using the Canin record from Colucci & Guglielmin (2015). This was possible, as the correlation between temperatures at the local weather stations and the Canin is statistically significant (for Baldass $R=0.95$ and for Malga Valine $R=0.87$; Fig. 3). The calculated 2010-2020 MSAT at Canin is 2.2°C higher than the average between 1961 and 1990, therefore this value was added to the 2010-2020 MSAT of Baldass and Malga Valine to obtain the 1961-1990 value.

The results from ELAs calculation were then used to reconstruct the paleoclimatic conditions during the LGM and Late Glacial stadials. At first, paleoprecipitation was assumed to be equal to present-day records and summer temperatures at the ELA were calculated using the following equation from Ohmura & Boettcher (2018):

$$Pa = 5.87 T_{sum}^2 + 230 T_{sum} + 966 \quad (1)$$

S.E. = 648 mm

where Pa is annual precipitation (mm) and T_{sum} is summer (JJA) air temperature ($^{\circ}\text{C}$). Applying a summer environmental lapse rate of $0.65^{\circ}\text{C } 100^{-1} \text{ m}$, representative for the greater Alpine region (Rolland, 2003; Rubel et al., 2017), we calculated the temperature differences from the modern local weather stations. This procedure was equally repeated for different precipitation scenarios, ranging from -30% to +30% of the present-day value.

When comparing ELAs of paleoglaciers to present climatic conditions, all calculated values were assumed to represent environmental ELAs (envELA; Žebre et al., 2020). The envELA is the theoretical altitude at which a glacier can form and does not consider the effects of shading, avalanching, snow drifting, glacier geometry or debris-cover (Anderson et al., 2018). In the Alps it was found to be ~75-150 m higher than the regional effective ELA (effELA; Žebre et al., 2020), which accounts for these topographic effects when averaged over a longer climatic period (e.g., 15-30 years).

4. THE PLEISTOCENE DEPOSITS IN THE SILISIA VALLEY

Along the Silisia Valley, and on the northern side of Mount Raut, Pleistocene deposits are scattered; they can be lithologically grouped into breccias, gravels, conglomerates and diamictons. Some of the deposits recorded in the old geological map (Zenari, 1929) are presently drowned by the Ca' Selva Lake. Many outcrops are visible along road cuts. An overview about the areas mentioned in the description and the location of the deposits is given in a photograph in Fig. 4A and in a cross-profile through the Silisia Valley (Fig. 5).

4.1. Breccias, gravels and conglomerates

Conglomerates are located in several sectors of the valley. The cementation of these deposits is strong and some of them show karstic dissolution structures (Fig. 4B). The conglomerates are made of clast-supported gravels, crudely bedded to horizontally bedded, and characterized by sub-rounded clasts of limestones, dolostones and cherts (red and black), pointing to a provenance from the upper catchment of the Silisia Valley. Lateral interfingering with angular breccias is visible and suggests the occurrence of local alluvial or talus deposits. Conglomerates mainly crop out in three locations: Chiavalot, Sarazin ridge, and Selva (see Figs. 2, 4A and 5). In the Chiavalot area, conglomerates are about 40 m thick, with the basal boundary on the bedrock at 900-910 m, and the rim of the Chiavalot cliff at 950 m, around 400 m above the lake. The deposits are karstified and deeply cut by local stream incisions. On the Sarazin ridge, the conglomerate and breccias are visible along the roadcut (Fig. 4C), clasts of conglomerates (i.e., the unit preserved at Chiavalot) are included indicating the erosion of an older conglomerate body. The topmost conglomerates are at 775 m and the basal boundary can be observed at ca. 670 m, suggesting the presence of a former valley fill with an overall thickness of around 100 m. The breccia/conglomerate body is locally weakly cemented and intersected by several joints that can be likely ascribed to tectonic activity. Similar deformed breccias are located at about 610 m, along the main road at the southern side of the lake. A small outcrop of conglomerates is located on the southern tip of the ridge separating the village of Selva from the valley gorge downstream of the dam (Fig. 2). This deposit is only a few meters thick and lays on top of the bedrock on the western slope of the ridge. Upstream the present lake, at Stua, a succession of gravels and sandy gravels crops out (D'Agostina, 2010); these are bedded and gently inclined ($10\text{-}20^{\circ}$) downstream and show a thickness of about 10 m. They are interpreted as related to a fan delta body.

4.2. Diamictons

Along the road flanking the southern side of the Ca' Selva Lake, sub-rounded boulders are common and outcrops of diamicton, matrix-supported, with striated clasts occur frequently. Clasts are sub-angular to sub-rounded and clast petrography is mostly made of dolostones and limestones, with angular chert clasts (red and black). Because of their sedimentary properties, these deposits were ascribed to glacial deposition.

In detail, the westernmost outcrop of these diamictons along the lake corresponds to the moraine of Case Val Bassa at the elevation of 520 m. The moraine ridge is ca. 300 m long and located on the left side of the valley outlet between elevations 575 m and 500 m. It contains mostly sub-angular to sub-rounded, large dolostone and limestone boulders, few of which show striations. The overall thickness of the deposit is about 25 m. A similar diamicton crops out at the outlet of the Basson Valley at an elevation of ca. 500 m (Fig. 4E). It is also associated to a left lateral moraine, that is well preserved close to the lake and partly covered by talus. The right moraine flank has been remodelled and a cluster of



Fig. 4 - Plate of pictures taken during field work. A. View across the Lake Ca' Selva towards the valley mouths of the Valine (in the foreground), Basson and Bassa (hidden). Visible are also the Chiavalot cliff and the Sarazin Ridge, two locations at which thick conglomerate bodies are cropping out. B. Strongly cemented conglomerate from the Chiavalot. C. Stratified conglomerate along the roadcut at the Sarazin Ridge. D. The glacial diamicton at Case Staleros. E. Glacial diamicton at the mouth of the Basson Valley. F. View towards the upper Valine catchment and the Malga Valine, where the terminal moraine is marked by red dashed line. G. The terminal moraine ridges at Casera Valine with a large limestone erratic in the foreground situated on the moraine crest. H. Fluted moraines in the upper Valine catchment.

big boulders is now partially drowned by the lake (D'Agostina, 2010). As well, in the lower reach of the Valine Valley, matrix-supported diamicton, with big boulders and mostly sub-angular to sub-rounded dolostone and limestone clasts, crops out close to the Sarazin ridge, at about 600 m. Here, however, it is not associated to a clear landform, as it is the case for the outlets of Basson and Bassa valleys outlets.

A thick unit of diamicton is located at Case Staleros, east of the Ca' Selva dam, where it lays on top of the bedrock at an elevation of 530 m. It consists of matrix-supported diamicton, embedding big boulders and striated clasts (Fig. 4D). Clasts are angular to sub-rounded; clast petrography indicates dominant dolostones and limestones (mostly sub-rounded), with minor amounts of cherts. The matrix is sandy and the deposit is normally consolidated and weakly and spotty cemented. The visible thickness of the deposit is about 25 m and it is associated to the moraine ridge of Stavoli Staleros. Downstream from this moraine along the Silisia Valley, no glacial deposits have been observed.

Several clusters of moraine ridges can also be recognized in the upper sectors of the Basson and Valine narrow valleys. A wide set of arch-shaped terminal moraines, up to 5 m high, is located in the Valine Valley at Casera Valine (1330 m) and forms a large flat area on the back (Fig. 4F and 4G). The moraines are made of diamicton, mostly characterized by angular/subangular boulders in a sandy matrix. On the back of the frontal moraines two longitudinal ridges made of boulders can be ascribed to fluted moraines on the base of their downvalley elongated morphology (Fig. 4H). In the Basson Valley, ending with the Mount Raut headwall, two separated sets of moraines can be distinguished. The first set is located at 1050 m and consists of mainly of lateral moraines, while the frontal moraines are flat and have been reshaped by local drainage. The second set of moraines is located upstream in the valley between 1425 and 1600 m. These moraines are elongated lateral ridges, while the frontal sector is characterized by scattered boulders in a flat area at about 1400 m.

5. GLACIER RECONSTRUCTIONS

Given the abundance of glacial landforms and sediments containing clast lithologies of local provenance, it can be concluded that the northern side of Mount Raut was covered by a glacial system that remained independent from the Alpine glacier network. No dating is available for these glacial features. Nevertheless, it is possible to attribute them to glacial advances during the Last Glacial Maximum and subsequent Late Glacial stages, considering the absence of deep weathering and cementation that would typically characterize sediments related to prior glaciations. The only exception is the diamicton at Stavoli Staleros, which is interpreted as a pre-LGM glacial deposit. This is both due to its sedimentary properties (i.e., spotty cementation) and its overall position in the valley system, more than 150 m high above the present course of the Silisia Stream (see Figs. 4A and 5). An interpretation of the Staleros moraine as an LGM ice-front would require both exceedingly thick ice in the Silisia Valley and extremely high post-glacial erosion rates, both of which are not compatible with field evidence and glacier modeling.

The LGM glacial network was therefore reconstructed basing on the presence of glacial deposits and frontal moraines that are present at the outlets of the Bassa, Basson and Valine valleys. Detailed information on the reconstructed glaciers, including calculated ELAs for the LGM and Late Glacial stadials is presented in Tab. 1. The ELAs calculated for AABRs of 1.56 and 1.29 do not show large differences, and are within the error range generally expected for ELA reconstructions (Oien et al., 2021). There is also a good agreement with the calculations using an AAR value of 0.65, while the global median of 0.58 results in slightly higher ELAs. Although for the smaller Late Glacial stages also AAR values of 0.5 and 0.7 yield reasonable estimates, a change in these ratios for the LGM results in a large shift of the calculated ELA (AAR 0.5 =1480 m; AAR 0.7 =1140 m). This is likely due to the particular hypsometry of the Mount Raut glacier during the LGM, with very steep and narrow valleys present in proximity to the ELA. Because of these potential complications, all ELAs in the following

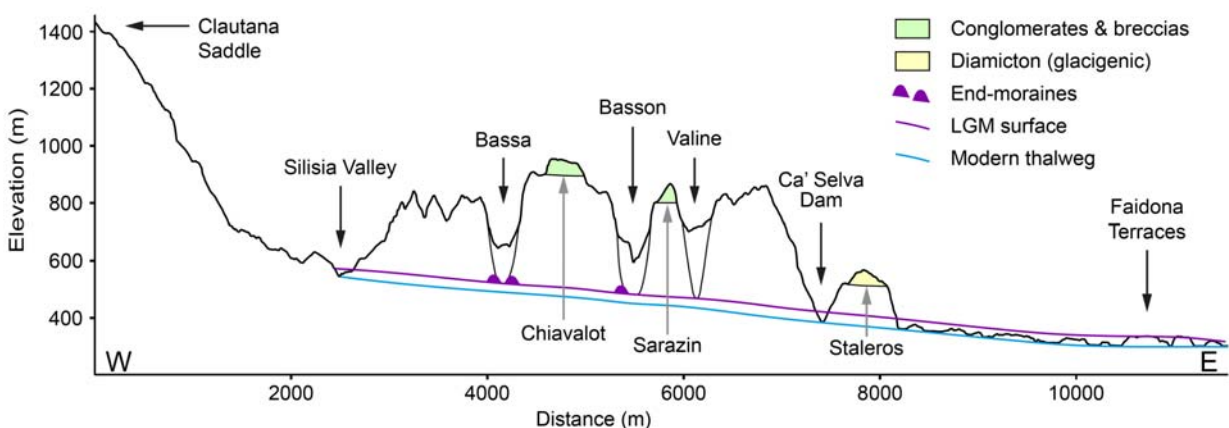


Fig. 5 - Cross-profile through the Silisia Valley including the major side valleys and sedimentary units discussed in the text. For the location of the profile see Fig. 1.

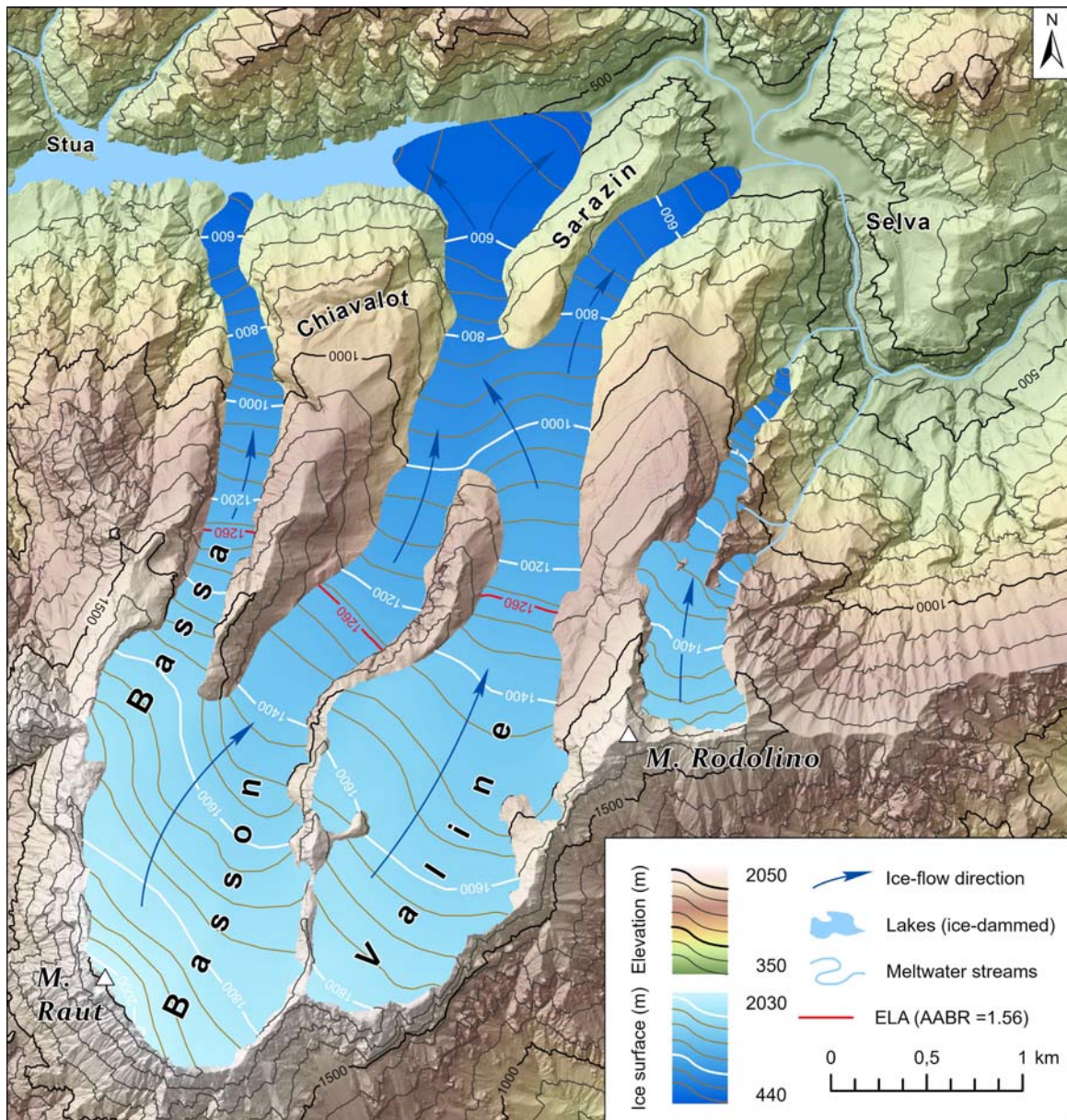


Fig. 6 - The reconstructed glacial system of Mount Raut during the LGM (ELA = 1260 m).

paragraphs and in the climatic interpretations are reported using the AABR-method with the global median value of 1.56 (Oien et al., 2021).

5.1. The Mount Raut glacier during the Last Glacial Maximum

During the LGM, the glacial system of the Mount Raut had an ELA of 1260 m and covered an area of approximately 7 km² with glacier tongues extending into all three main valleys on its northern side (Fig. 6). Ice was accumulating on the high-altitude plateaus of the Basson and Valine catchments up to an altitude of ca. 2030 m. A smaller accumulation area was also located at the head of the Bassa Valley, although this tributary probably received part of its ice through transfluence

from the neighboring Basson catchment. From the plateaus, the ice was flowing northwards, constrained within the narrow glacial valleys. In the Bassa Valley, the maximum ice extent during the LGM is clearly delineated by a frontal moraine ridge, situated at an altitude of 520 m, indicating that the glacier advance stopped just before reaching the E-W trending Silisia Valley. In contrast, the glacier tongue coming from the Basson Valley advanced further downstream, as shown by the presence of glacial diamicton and scattered boulders around the flat valley mouth. The larger extent of this tributary can be explained both by the high elevations of the Basson plateau, and by the fact that it received additional input from the Valine catchment further downstream. The infilling of the valley mouth with glacier ice likely led to a damming

of the Silisia Stream, a hypothesis which is corroborated by the presence of fan delta deposits further upstream (D'Agostina, 2010).

In the lower Valine Valley, clear geomorphological evidence in the form of a frontal moraine is lacking. However, scattered occurrence of glacial deposits and large boulders at an altitude of 500-600 m suggests that also this tongue extended down towards the valley mouth. The frontal moraine system of this lobe might presently be covered by the Ca' Selva Lake or, alternatively, might have already been eroded by the Silisia Stream before the construction of the dam. In addition, a smaller LGM glacier developed in the cirque northwest of Mount Rodolino (Fig. 6), which remained independent from the Mount Raut glacial system. However, no clear indication of its frontal position was found, which is at least partly due to the steepness of the terrain in this area.

5.2. The Valine and Basson glaciers during the Late Glacial

After the LGM, the glaciers of the Mount Raut retreated into the higher parts of their catchments. Evidence for phases of glacier stabilization or re-advance during this time can be found as series of moraines both in the Valine and the Basson valleys. In the Valine Valley, several well-defined moraine ridges are located at an elevation of around 1330 m, delimiting a small glacier (surface area of ca. 0.9 km²) with an ELA of 1570 m (Fig. 7A). Due to its higher catchment, the Basson glacier must have still had a larger extent during this time, with its front potentially stabilizing at an altitude of ca. 1050 m. Although patches of glacial deposits and moraine ridges were found here in a lateral position, an evident frontal system is lacking, and it is not clear if these deposits relate to a distinct Late Glacial advance or can be ascribed to the downwasting of the LGM glacier.

Conversely, in the Basson Valley a second set of moraines can be found stretching down to an altitude of ca. 1400 m, indicating a later phase of glacier stabilization during the Late Glacial. The Basson glacier reconstructed for this stage covered an area of ca. 1.2 km² and its ELA was calculated at 1740 m (Fig. 7B). At the

same time, the glacier in the Valine must have almost entirely disappeared or was preserved only as a small niche glacier or firn field, which could also explain the absence of depositional features on the upper Valine plateau.

6. DISCUSSION

6.1. The Pleistocene evolution of the Silisia Valley and the Mount Raut paleoglaciers

The southern sector of the Meduna catchment has been affected by important drainage changes since the Messinian, and during the Pleistocene, several alluvial sedimentary units were deposited in the lower reach of the valley (Monegato & Poli, 2015). The tectonic evolution of the south-eastern Alps (Poli et al., 2009, 2021) has driven these changes. In this perspective, it can be assumed that also the two conglomerate units, at Chiavalot and Sarazin, are linked to the evolution of the Silisia Valley and the ongoing incision and infill during Plio(?)–Pleistocene time. The differences in cementation and weathering degree, also considering the presence of conglomerate pebbles in the Sarazin body, then point to different sedimentation of these units in events that pre-date the last sedimentation phase related to the LGM and Late Glacial. Considering the difference in elevation between Chiavalot and Sarazin of more than 200 m, and the location of the Chiavalot in the footwall of the Silisia thrust, the progressive incision of the Silisia Stream probably felt the effect of the general uplift in this sector of the Carnic Prealps, which is related to the frontal thrusts of the eastern Southalpine south-eastern Alpine chain (Poli et al., 2009, 2021). In this respect, the Silisia Valley and the Mount Raut lie on the hanging wall of the Periadriatic thrust (Carulli et al., 2000), while the lower Meduna valley sedimentary stack is located between the Periadriatic thrust and the M. Jouv-Maniago thrust system. Three tectonic phases were described in the frontal sector of the Carnic Prealps (Caputo et al., 2010; Monegato & Poli, 2015), pointing to a potential enhancement of fluvial incision during uplift phases, especially along the major cataclastic belts related to the tectonic structures. The infilling phases of such narrow tributary valleys can be ascribed to glacial damming or

Time period	Glacier	Surface area [km ²]	Max. Elevation [m a.s.l.]	Min. Elevation [m a.s.l.]	ELA AAR [m]				ELA AABR [m]	
					0.5	0.58	0.65	0.7	1.29	1.56
Last Glacial Maximum (LGM)	Monte Raut	7	2063	439	1480	1380	1250	1140	1300	1260
	Valine tributary	2.8	1850	445						
	Basson tributary	3.3	2063	439						
	Bassa tributary	0.9	1769	538						
	Monte Rodolino	0.7	1610	624						
Late Glacial Stage 1	Valine	0.9	1823	1347	1620	1580	1560	1540	1580	1570
	Basson	1.8	2063	1052						
Late Glacial Stage 2	Valine	0.3	1823	1611						
	Basson	1.2	2063	1363	1790	1770	1740	1720	1750	1740

Tab. 1 - Characteristics of the reconstructed glaciers on the northern side of Mount Raut for the LGM and two Late Glacial stages, including ELAs calculated for several AABRs and AARs. In red, hypothetical reconstructions due to lack of geomorphological evidence

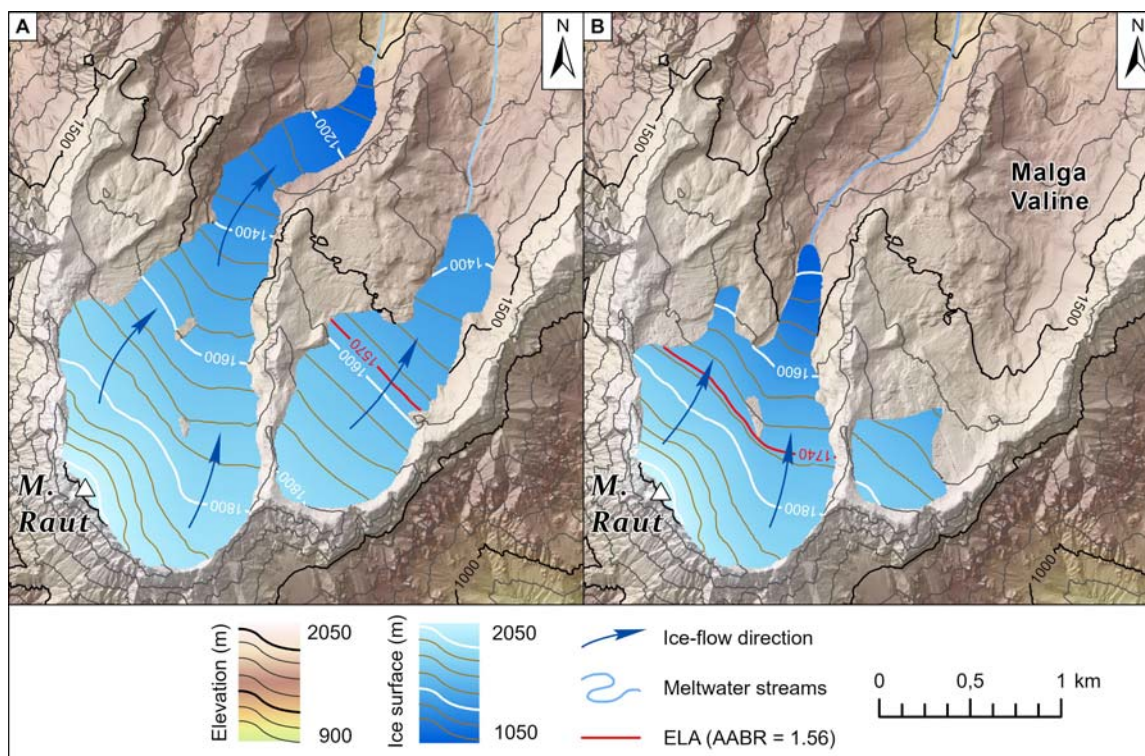


Fig. 7 - The Valine and Basson glaciers during the Late Glacial. A. Late Glacial stage 1 (ELA = 1570 m). B. Late Glacial stage 2 (ELA = 1740 m).

landslide damming. In this perspective, the Chiavalot unit represents the oldest sedimentary infill of the valley, which can be linked to the karstified conglomerates of the lower Meduna valley (Monegato & Poli, 2015). The deepening of the valley of about 200 m occurred before the deposition of the Sarazin unit and suggests that an uplift phase likely took place in the lower Pleistocene. The difference in elevation of about 170 m from the basal boundary of the Sarazin unit to the LGM deposits also indicates this post-depositional uplift. This influenced the deep incision downstream of the dam, which led to the abandonment of the path through Selva and the preservation of the glacial deposits of Staleros. A similar deepening characterizes also the Meduna Valley, which was later filled by lacustrine deposits (Venzo et al., 1975; Cavallin & Martinis, 1981). The Staleros unit itself can most likely be ascribed to a Middle Pleistocene ice advance, even if no chronological data are available. In the lower Meduna Valley, old alluvial terraces (Monegato & Poli, 2015) may represent its outwash deposition.

During the LGM, glaciers in the Valine, Basson and Bassa catchments advanced for the last time beyond their valley mouths, leading to the deposition of frontal moraines and glacial sediments and at least temporarily to a damming of the Silisia Valley upstream. The well-preserved fluvial terraces of Faidona (Cavallin & Martinis, 1981), at the confluence with the Meduna Valley, can probably be ascribed to deposition by meltwaters originating from the glacial system during this time. From the position of the moraine ridges, however, it can clearly be established that the Raut paleoglacier

itself never merged with the glacial system of the Meduna Valley, as it was sometimes reported in previous studies (Gortani, 1959; Ehlers & Gibbard, 2004). Regionally, the first culmination of the LGM advance has been dated to around 26.5 to 23 cal ka BP, with a later pulse occurring at 22 cal ka BP (Tagliamento end-moraine system, Monegato et al., 2007; Fontana et al., 2014). This later stage also corresponds to the phase of maximum aggradation in the Meduna alluvial fan (Avigliano et al., 2002). Although no numerical dating is available for the Mount Raut, we hypothesize that the advance of the glacial system during the LGM probably took place during the same time span, considering the similar climatic setting to the Meduna and Tagliamento catchments.

Following the downwasting of the LGM glaciers, two distinct advances of the Basson and Valine valley glaciers occurred during the Late Glacial. Such stages of stabilization have been equally recognized in parts of the Carnic Alps and Julian Prealps (Discenza, 2004; Colucci et al., 2014) and the Chiampon-Cuel di Lanis ridge (Monegato, 2012). In the latter case, these glaciers exhibit an ELA ca. 250 to 350 m higher with respect to the LGM, which matches the calculations for Late Glacial stage 1 (LG1) in the Valine (ELA raising of ca. 330 m). Even if this may point to a common climatic driver for the glacier advance, a detailed chronology for the ice-decay in the south-eastern Alps is still lacking, which hampers comparisons between different mountain ranges or a correlation to one of the established Late Glacial stadials in other sectors of the Alps (e.g., Ivy-Ochs et al., 2008).

6.2. Paleoclimate reconstructions

The calculated ELA of 1260 m for the LGM glacial system is among the lowest reported for the southern fringe of the Alps so far. It corresponds best with those calculated from other areas in the south-eastern part of the range, such as the Julian Prealps (ELAs =1128-1190 m, Monegato, 2012), or the Trnovski gozd in the Slovenian Dinaric Mountains (ELA =1240, Žebre et al., 2014). Already at Mount Grappa, ca. 75 km further west, ELAs are reported to be around 150-200 m higher than at Mount Raut (Carraro & Sauro, 1979; Baratto et al., 2003). The values increase even further towards the central southern Alps (ELA =1535 m; Forno et al., 2010) or the Maritime Alps (ELA =1850 m; Federici et al., 2012), indicating that an east-west ELA-gradient probably prevailed along the southern fringe of the Alps during the LGM.

Present (2010-2020) MSAT in Baldass and Malga Valine, which are closer in respect to the Pala d'Altei station, are at 12.6°C and 14.8°C, respectively. Given the ELA of 1260 m, and assuming present-day precipitation, our calculations suggest that, compared to the period 1961-1990, MSAT in the Mount Raut area was depressed by around 9.4°C or 8.5°C during the LGM, by 7.1 or 6.2 °C during the LG1, and by 6.1 or 5.3°C during the LG2, respectively ($\sigma = \pm 2.2^\circ\text{C}$). The results for the LGM are consistent with regional models of atmospheric circulation (Kuhlemann et al., 2008) and also with chironomid-based July temperatures reconstructed at Lago della Costa (Euganean Hills, Samartin et al., 2016). With different precipitation scenarios ($\pm 30\%$ of the present-day value, see Tab. 2, 3, 4), MSAT depressions vary between 6.2°C (7.0°C, respectively) and 11.6°C (10.8°C, respectively). With a further reduction in precipitation, reconstructed temperatures are not compatible anymore with the aforementioned calculations from other proxies. This indicates that the LGM climate in the south-eastern Alps was very likely characterized by high precipitation throughout the whole LGM. These high amounts of precipitation, especially during autumn and winter (Spötl et al., 2021), allowed glaciers to expand to lower elevations as in other parts of the southern Alps and today it still ensures the preservation of very small glaciers in parts of the Carnic and Julian Alps (Colucci et al., 2021).

7. CONCLUSION

New evidence for the Pleistocene evolution of Mount Raut and the neighboring Silisia Valley is presented in this study, basing on mapping and description of Quaternary sediments and landforms. Detailed studies concerning the Quaternary deposits and landforms in the area were previously still lacking. Two bodies of conglomerates were found and they have been related to the recurring infill and incision of the Silisia Valley during Plio(?)–Pleistocene times, probably driven partly by climatic fluctuations and partly by tectonic uplift phases of the south-eastern Alps. Series of moraine ridges and glacial deposits are mainly related to glacier advances during the LGM and following Late Glacial stages.

In the south-eastern part of the European Alps,

MAP	MSAT depression LGM		MSAT depression LGM	
	Baldass - 1817 m asl		Malga Valine - 1346 m asl	
1961-2000	2010-2020	1961-1990	2010-2020	1961-1990
0%	-11,6	-9,4	-10,7	-8,5
-5%	-11,9	-9,7	-11,1	-8,9
-10%	-12,2	-10,0	-11,4	-9,2
-15%	-12,5	-10,3	-11,7	-9,5
-20%	-12,9	-10,7	-12,0	-9,8
5%	-11,2	-9,0	-10,4	-8,2
10%	-10,9	-8,7	-10,1	-7,9
15%	-10,6	-8,4	-9,8	-7,6
20%	-10,9	-8,7	-10,1	-7,9

Tab. 2 - MSAT depression calculated for the LGM, assuming different MAP scenarios.

MAP	MSAT depression LG1		MSAT depression LG1	
	Baldass - 1817 m asl		Malga Valine - 1346 m asl	
1961-2000	2010-2020	1961-1990	2010-2020	1961-1990
0%	-9,3	-7,1	-8,4	-6,2
-5%	-9,6	-7,4	-8,8	-6,6
-10%	-9,9	-7,7	-9,1	-6,9
-15%	-10,2	-8,0	-9,4	-7,2
-20%	-10,6	-8,4	-9,7	-7,5
5%	-8,9	-6,7	-8,1	-5,9
10%	-8,6	-6,4	-7,8	-5,6
15%	-8,3	-6,1	-7,5	-5,3
20%	-8,6	-6,4	-7,8	-5,6

Tab. 3 - MSAT depression calculated for the Late Glacial stage 1, assuming different MAP scenarios.

MAP	MSAT depression LG2		MSAT depression LG2	
	Baldass - 1817 m asl		Malga Valine - 1346 m asl	
1961-2000	2010-2020	1961-1990	2010-2020	1961-1990
0%	-8,3	-6,1	-7,5	-5,3
-5%	-8,6	-6,4	-7,8	-5,6
-10%	-8,9	-6,7	-8,1	-5,9
-15%	-9,3	-7,1	-8,4	-6,2
-20%	-9,6	-7,4	-8,8	-6,6
5%	-8,0	-5,8	-7,1	-4,9
10%	-7,6	-5,4	-6,8	-4,6
15%	-7,3	-5,1	-6,5	-4,3
20%	-7,6	-5,4	-6,8	-4,6

Tab. 4 - MSAT depression calculated for the Late Glacial stage 2, assuming different MAP scenarios.

several small mountain glaciers remained independent from the large alpine ice-streams throughout the late Pleistocene cold phases, including the Last Glacial Maximum, one of which was located on the northern side of Mount Raut (Carnic Prealps, NE Italy). The reconstruction of these glaciers and their ELAs reveals important information about the past climate.

Our investigation shows that the LGM glacial system of the Mount Raut covered an area of ca. 7 km². Its ELA (AABR) was calculated at 1260 m. Assuming levels of precipitation similar to today, an LGM MSAT depression of 8.5 or 9.4°C ($\sigma = \pm 2.2^\circ\text{C}$) was calculated in re-

spect to two recent (1960-1990) climatic records in the area. During the Late Glacial, glaciers were confined in the upper parts of their catchments, intermitted by two distinct phases of glacier stabilization, the first at which glaciers had an ELA of 1590 m (corresponding to an MSAT lowering of 6.2 or 7.1°C) and the second with an ELA of 1740 m (MSAT lowering of 5.3 or 6.1°C).

These calculations are generally in line with regional circulation models, indicating that glaciers in the south-eastern Alps received high amounts of precipitation throughout the LGM. However, further research is needed to better understand the paleoclimatic evolution in the south-eastern Alps during the last glacial cycle, by integrating glacier-based climate reconstructions with numerical dating methods to better constrain the LGM and Late Glacial advances.

ACKNOWLEDGEMENTS

We want to thank G. Marcato and M. Spagnolo for discussions and input, the Forestal Service of Region FVG for access permissions of the area. The reviews provided by A. Ribolini and H. Kerschner greatly improved our manuscript. We also thank A. Fontana (A.E.) for his comments.

REFERENCES

- Anderson R.S., Anderson L.S., Armstrong W.H., Rossi M.W., Crump S.E. (2018) - Glaciation of alpine valleys: The glacier - debris-covered glacier - rock glacier continuum. *Geomorphology*, 311, 127-142. Doi: 10.1016/j.geomorph.2018.03.015
- Avigliano R., Calderoni G., Monegato G., Mozzi P. (2002) - The late Pleistocene-Holocene evolution of the Cellina and Meduna alluvial fans (Friuli, NE Italy). *Memorie Società Geologica Italiana*, 57, 133-139.
- Bacon S.N., Chinn T.J., van Dissen R.J., Tillinghast S.F., Goldstein H.L., Burke R.M. (2001) - Paleoequilibrium line altitude estimates from late Quaternary glacial features in the Inland Kaikoura Range, South Island, New Zealand. *New Zealand Journal of Geology and Geophysics*, 44(1), 55-67. Doi: 10.1080/00288306.2001.9514922
- Baratto A., Ferrarese F., Meneghel M., Sauro U. (2003) - La ricostruzione della glaciazione Wurmiana nel Gruppo del Monte Grappa (Prealpi Venete). In: *Risposta dei processi geomorfologici alle variazioni ambientali*. (Ed. by Biancotti A., Motta M.). Brigati G., Genova, 67-77.
- Beniston M. (2005) - Mountain Climates and Climatic Change: An Overview of Processes Focusing on the European Alps. *Pure and Applied Geophysics*, 162, 1587-1606. Doi: 10.1007/s00024-005-2684-9
- Beniston M. (2006) - Mountain weather and climate: A general overview and a focus on climatic change in the Alps. *Hydrobiologia*, 562, 3-16. Doi: 10.1007/s10750-005-1802-0
- Benn D.I., Hulton N.R.J. (2010) - An Excel™ spreadsheet program for reconstructing the surface profile of former mountain glaciers and ice caps. *Computers & Geosciences*, 36(5), 605-610. Doi: 10.1016/j.cageo.2009.09.016
- Brædstrup C.F., Egholm D.L., Ugelvig S.V., Pedersen V.K. (2016) - Basal shear stress under alpine glaciers: insights from experiments using the iSOSIA and Elmer/Ice models. *Earth Surface Dynamics*, 4(1), 159-174. Doi: 10.5194/esurf-4-159-2016
- Caputo R., Poli M.E., Zanferrari A. (2010) - Neogene-Quaternary tectonic stratigraphy of the eastern Southern Alps, NE Italy. *Journal of Structural Geology*, 32(7), 1009-1027. Doi: 10.1016/j.jsg.2010.06.004
- Carraro F., Polino R. (1976) - Vistose deformazioni in depositi fluvio-lacustri quaternari a Ponte Racli (Valle del T. Meduna - Prov. di Pordenone). *Quaderni Gruppo di Studio Quaternario Padano*, 3, 77-88.
- Carraro F., Sauro U. (1979) - Il Glacialismo "locale" Wurmiano del Massiccio del Grappa (Province di Treviso e di Vicenza). *Geografia Fisica e Dinamica Quaternaria*, 2(1), 6-16.
- Carulli G.B., Cozzi A., Longo Salvador G., Pernarcic E., Podda F., Ponton M. (2000) - Geologia delle Prealpi Carniche. With enclosed Carta Geologica delle Prealpi Carniche, scala 1:50.000. *Pubbl. no 44, Edizioni Museo Friulano Storia Naturale, Udine*, 47 pp.
- Carulli G.B., Podda F., Venturini C., Zanferrari A., Cucchi F., Monegato G., Nicolich R., Paiero G., Piano C., Slejko D., Tunis G., Zanolla C. (2006) - Carta Geologica del Friuli Venezia Giulia (Scala 1:150.000). Edizioni S.EL.CA., Firenze.
- Castiglioni B. (1940) - L'Italia nell'età quaternaria. Carta alla scala 1:200.000. *Atlante Fisico-Economico d'Italia, TCI, Milano*.
- Castiglioni G.B. (2004) - Quaternary glaciations in the eastern sector of the Italian Alps. In: *Quaternary Glaciations - Extent and Chronology-Part I: Europe* (Ed. by Ehlers J., Gibbard P.L.). Elsevier, 209-215.
- Cavallin A., Martinis B. (1981) - Il bacino lacustre della conca di Tramonti (Prealpi Carniche). *Alto*, 63, 1-17.
- Clark C.D., Chiverrell R.C., Fabel D., Hindmarsh R.C.A., Ó Cofaigh C., Scourse J.D. (2021) - Timing, pace and controls on ice sheet retreat: an introduction to the BRITICE-CHRONO transect reconstructions of the British-Irish Ice Sheet. *Journal of Quaternary Science*, 36(5), 673-680. Doi: 10.1002/jqs.3326
- Colucci R.R., Monegato G., Žebre M. (2014) - Glacial and proglacial deposits of the Resia Valley (NE Italy): new insights on the onset and decay of the last Alpine Glacial Maximum in the Julian Alps. *Alpine and Mediterranean Quaternary*, 27(2), 85-104.
- Colucci R.R., Guglielmin M. (2015) - Precipitation-temperature changes and evolution of a small glacier in the southeastern European Alps during the last 90 years. *International Journal of Climatology*, 35(10), 2783-2797. Doi: 10.1002/joc.4172
- Colucci R.R., Žebre M., Torma C.Z., Glasser N.F., Maset E., Del Gobbo C., Pillon S. (2021) - Recent

- Increases in Winter Snowfall Provide Resilience to Very Small Glaciers in the Julian Alps, Europe. *Atmosphere*, 12(2), 263.
Doi: 10.3390/atmos12020263
- Crespi A., Brunetti M., Lentini G., Maugeri M. (2018) - 1961-1990 high-resolution monthly precipitation climatologies for Italy. *International Journal of Climatology*, 38(2), 878-895.
Doi: 10.1002/joc.5217
- Cucato M. (2007) - La successione continentale plioce-nico?-quaternaria. In: Note Illustrative della Carta Geologica d'Italia alla scala 1:50.000: Foglio 082 "Asiago" (Ed. by Barbieri, G., Grandesso, P.). APAT e Dipartimento Difesa del suolo e Servizio Geologico d'Italia, Roma, Italia, pp. 60-94.
- D'Agostina N. (2010) - Stima dell'interramento di un bacino artificiale mediante l'utilizzo del modello multiparametrico Gavrilovich-Zemlich. Tesi di Laurea inedita, Università degli Studi di Trieste, 101 pp.
- Dal Piaz G.V., Bistacchi A., Massironi M. (2003) - Geological outline of the Alps. *Episodes*, 26/3, 174-179.
- Discenza K. (2004) - Evoluzione tardo quaternaria delle Alpi meridionali orientali. Tesi di Dottorato di ricerca, Università di Bologna.
- Ehlers J., Gibbard P. L. (2004) - Quaternary glaciations-extent and chronology: part I: Europe. Elsevier, Amsterdam.
- Federici P.R., Granger D.E., Ribolini A., Spagnolo M., Pappalardo M., Cyr A.J. (2012) - Last Glacial Maximum and the Gschnitz stadial in the Maritime Alps according to ¹⁰Be cosmogenic dating. *Boreas*, 41 (2), 277-291.
Doi: 10.1111/j.1502-3885.2011.00233.x
- Fontana A., Monegato G., Devoto S., Zavagno E., Burla I., Cucchi F. (2014) - Evolution of an Alpine glacio-fluvial system at the LGM decay: the Cormor megafan (NE Italy). *Geomorphology*, 204, 136-153.
Doi: 10.1016/j.geomorph.2013.07.034
- Forno M.G., Gianotti F., Racca G. (2010) - Significato paleoclimatico dei rapporti tra il glacialismo principale e quello tributario nella bassa Valle della Dora Baltea. *Il Quaternario*, 23(1), 105-124.
- Gortani M. (1959) - Carta della glaciazione würmiana in Friuli. *Rendiconti Atti della Accademia delle scienze dell'Istituto di Bologna*, 11(6), 1-11.
- Hofmann F.M., Alexanderson H., Schoeneich P., Mertes J.R., Léanni L. (2019) - Post-Last Glacial Maximum glacier fluctuations in the southern Écrins massif (westernmost Alps): insights from ¹⁰Be cosmic ray exposure dating. *Boreas*, 48(4), 1019-1041.
Doi: 10.1111/bor.12405
- Hughes A.L.C., Gyllencreutz R., Lohne Ø.S., Mangerud J., Svendsen J.I. (2016) - The last Eurasian ice sheets-a chronological database and time-slice reconstruction, DATED-1. *Boreas*, 45(1), 1-45.
Doi: 10.1111/bor.12142
- Isotta F.A., Frei C., Weigluni V., Tadić M.P., Lassègues P., Rudolf B., Pavan V., Cacciamani C., Antolini G., Ratto S.M., Munari M., Micheletti S., Bonati V., Lussana C., Ronchi C., Panettieri E., Marigo G., Vertačnik G. (2014) - The climate of daily precipitation in the Alps: development and analysis of a high resolution grid dataset from pan-Alpine rain-gauge data. *International Journal of Climatology*, 34, 1657-1675.
Doi: 10.1002/joc.3794
- Iverson N.R., Cohen D., Hooyer T.S., Fischer U.H., Jackson M., Moore P.L., Lappégard G., Kohler J. (2003) - Effects of Basal Debris on Glacier Flow. *Science*, 301(5629), 81-84.
Doi: 10.1126/science.1083086
- Ivy-Ochs S., Kerschner H., Reuther A., Preusser F., Heine K., Maisch M., Kubik P.W., Schlüchter C. (2008) - Chronology of the last glacial cycle in the European Alps. *Journal of Quaternary Science*, 23, 559-573.
Doi: 10.1002/jqs.1202
- Ivy-Ochs S., Monegato G., Reitner J.M. (2021) - Glacial landscapes of the Alps. In: *European Glacial Landscapes: Maximum Extent of Glaciations* (Ed. by Palacios D., Hughes P.D., García Ruiz J.M., de Andrés N.). Elsevier, Amsterdam, 115-121.
- Jouvet G., Seguinot J., Ivy-Ochs S., Funk M. (2017) - Modelling the diversion of erratic boulders by the Valais Glacier during the last glacial maximum. *Journal of Glaciology*, 63, 487-498.
Doi: 10.1017/jog.2017.7
- Kuhlemann J., Rohling E.J., Krumrei I., Kubik P., Ivy-Ochs S., Kucera M. (2008) - Regional synthesis of Mediterranean atmospheric circulation during the Last Glacial Maximum. *Science*, 321 (5894), 1338-1340.
Doi: 10.1126/science.1157638
- Monegato G., Ravazzi C., Donegana M., Pini R., Calderoni G., Wick L. (2007) - Evidence of a two-fold glacial advance during the last glacial maximum in the Tagliamento end moraine system (eastern Alps). *Quaternary Research*, 68(2), 284-302.
Doi: 10.1016/j.yqres.2007.07.002
- Monegato G. (2012) - Local glaciers in the Julian Prealps (NE Italy) during the last glacial maximum. *Alpine and Mediterranean Quaternary*, 25(1), 5-14.
- Monegato G., Poli M.E. (2015) - Tectonic and climatic inferences from the terrace staircase in the Meduna valley, eastern Southern Alps, NE Italy. *Quaternary Research*, 83(1), 229-242.
Doi: 10.1016/j.yqres.2014.10.001
- Nye J.F. (1952) - The mechanics of glacier flow. *Journal of Glaciology*, 2, 82-93.
Doi: 10.3189/S0022143000033967
- Ohmura A., Boettcher M. (2018) - Climate on the equilibrium line altitudes of glaciers: theoretical background behind Ahlmann's P/T diagram. *Journal of Glaciology*, 64(245), 489-505.
Doi: 10.1017/jog.2018.41
- Oien R.P., Rea B.R., Spagnolo M., Barr I.D., Bingham R.G. (2021) - Testing the area-altitude balance ratio (AABR) and accumulation-area ratio (AAR) methods of calculating glacier equilibrium-line altitudes. *Journal of Glaciology*.
Doi: <https://doi.org/10.1017/jog.2021.100>
- Paterson W.S.B. (1994) - *The Physics of Glaciers*: 3rd

- Edition. Pergamon, New York, pp. 480.
- Pellitero R., Rea B.R., Spagnolo M., Bakke J., Hughes P., Ivy-Ochs S., Lukas S., Ribolini A. (2015) - A GIS tool for automatic calculation of glacier equilibrium-line altitudes. *Computers & Geosciences*, 82, 55-62.
Doi: 10.1016/j.cageo.2015.05.005
- Pellitero R., Rea B.R., Spagnolo M., Bakke J., Ivy-Ochs S., Frew C.R., Hughes P., Ribolini A., Lukas S., Renssen H. (2016) - GlaRe, a GIS tool to reconstruct the 3D surface of palaeoglaciologists. *Computers & Geosciences*, 94, 77-85.
Doi: 10.1016/j.cageo.2016.06.008
- Penck A., Brückner E. (1901-1909) - *Die Alpen im Eiszeitalter*. Tauchnitz, Leipzig, Germany, pp. 1199.
- Poli M.E., Zanferrari A., Monegato G. (2009) - Geometria, cinematica e attività pliocenico-quadernaria del sistema di sovrascorimenti Arba-Ragogna (Alpi Meridionali orientali, Italia NE). *Rendiconti Online della Società Geologica Italiana*, 5, 172-175.
- Poli M.E., Falcucci E., Gori S., Monegato G., Zanferrari A., Affatato A., Baradello L., Bohm G., Dal Bo I., Forte E., Grimaz S., Marchesini A. (2021) - Paleoseismological evidence for historical ruptures along the Meduno Thrust (eastern Southern Alps, NE Italy). *Tectonophysics*, 818, 229071.
Doi: 10.1016/j.tecto.2021.229071
- Rea B.R. (2009) - Defining modern day Area-Altitude Balance Ratios (AABRs) and their use in glacier-climate reconstructions. *Quaternary Science Reviews*, 28(3-4), 237-248.
Doi: 10.1016/j.quascirev.2008.10.011
- Rea B.R., Pellitero R., Spagnolo M., Hughes P., Ivy-Ochs S., Renssen H., Ribolini A., Bakke J., Lukas S., Braithwaite R.J. (2020) - Atmospheric circulation over Europe during the Younger Dryas. *Science Advances*, 6(50), eaba4844.
Doi: 10.1126/sciadv.aba4844
- Rolland C. (2003) - Spatial and seasonal variations of air temperature lapse rates in Alpine regions. *Journal of Climate*, 16(7), 1032-1046.
Doi: 10.1175/1520-0442(2003)016<1032:SASVOA>2.0.CO;2
- Rubel F., Brugger K., Haslinger K., Auer I. (2017) - The climate of the European Alps: Shift of very high resolution Köppen-Geiger climate zones 1800-2100. *Meteorologische Zeitschrift*, 26(2), 115-125.
Doi: 10.1127/metz/2016/0816
- Samartin S., Heiri O., Kaltenrieder P., Kühl N., Tinner W. (2016) - Reconstruction of full glacial environments and summer temperatures from Lago della Costa, a refugial site in Northern Italy. *Quaternary Science Reviews*, 143, 107-119.
Doi: 10.1016/j.quascirev.2016.04.005
- Seguinot J., Ivy-Ochs S., Juvet G., Huss M., Funk M., Preusser F. (2018) - Modelling last glacial cycle ice dynamics in the Alps. *The Cryosphere*, 12(10), 3265-3285.
Doi: 10.5194/tc-12-3265-2018
- Spagnolo M., Ribolini A. (2019) - Glacier extent and climate in the Maritime Alps during the Younger Dryas. *Palaeogeography, Palaeoclimatology, Palaeoecology*, 536, 109400.
Doi: 10.1016/j.palaeo.2019.109400
- Spötl C., Koltai G., Jarosch A.H., Cheng H. (2021) - Increased autumn and winter precipitation during the Last Glacial Maximum in the European Alps. *Nature Communications*, 12, 1839.
Doi: 10.1038/s41467-021-22090-7
- Thorp P.W. (1991) - Surface profiles and basal shear stresses of outlet glaciers from a Late-glacial mountain ice field in western Scotland. *Journal of Glaciology*, 37(125), 77-88.
Doi: 10.3189/S0022143000042829
- Vai G.B., Cantelli, L. (Eds.) (2004) - *Litho-Palaeoenvironmental Maps of Italy during the Last Two Climatic Extremes*. Two Maps 1:1,000,000. 32° IGC publications, LAC, Bologna.
- van Husen D. (1987) - *Die Ostalpen und ihr Vorland in der letzten Eiszeit (Würm)*. Geologische Bundesanstalt, Vienna.
- Venturini C. (1985) - I depositi quaternari di Ponte Racli (PN, Prealpi Friulane). *Gortania, Atti Museo Friulano di Storia Naturale*, 7, 37-58.
- Venturini C., Discenza K., Astori A. (2013) - Sedimentologia e tettonica della successione clastica della Val Meduna (Prealpi Carniche, PN). *Gortania, Atti Museo Friulano di Storia Naturale*, 34, 51-78.
- Venzo G.A., Ulcigrai F., Cucchi F. (1975) - Studio geologico per i serbatoi di laminazione delle piene sul T. Meduna a La Clevata e a Colle. *Studi Trentini di Scienze Naturali Sez. A*, 52, 201-221.
- Višnjević V., Herman F., Prasicek G. (2020) - Climatic patterns over the European Alps during the LGM derived from inversion of the paleo-ice extent. *Earth and Planetary Science Letters*, 538, 116185.
Doi: 10.1016/j.epsl.2020.116185
- Žebre M., Stepišnik U., Kodelja B. (2014) - Traces of Pleistocene glaciation on Trnovski Gozd. *Dela*, 39, 157-170.
- Žebre M., Colucci R.R., Giorgi F., Glasser N.F., Racoviteanu A.E., Del Gobbo C. (2021) - 200 years of equilibrium-line altitude variability across the European Alps (1901-2100). *Climate Dynamics*, 56(3), 1183-1201.
Doi: 10.1007/s00382-020-05525-7
- Zenari S. (1929) - *Note illustrative della Carta Geologica delle Tre Venezie Foglio "Maniago"*. Ufficio Idrografico Regio Magistrato Acque di Venezia, Padova.